Brain, Behavior, & Immunity - Health 9 (2020) 100140

Contents lists available at ScienceDirect

Brain, Behavior, & Immunity - Health

journal homepage: www.editorialmanager.com/bbih/default.aspx

Full Length Article

An exploratory analysis of extracellular vesicle-associated and soluble cytokines in cancer-related fatigue in men with prostate cancer

Dilorom Sass [a,c], Wendy Fitzgerald [b], Jennifer J. Barb [d], Kevin Kupzyk [c], Leonid Margolis [b,*], Leorey Saligan [a]

[a] National Institute of Nursing Research, National Institute of Nursing Research, National Institutes of Health, Bethesda, MD, USA
[b] National Institute of Child Health and Human Development, Section on Intercellular Interactions, Eunice Kennedy-Shriver National Institute of Child Health and Human Development, National Institutes of Health, Bethesda, MD, USA
[c] University of Nebraska Medical Center, University of Nebraska Medical Center, Omaha, NE, 68105, USA
[d] Clinical Center, National Institutes of Health, Bethesda, MD, USA

ARTICLE INFO

Keywords:
Extracellular vesicles
Exosomes
Cytokines
Cancer-related fatigue

ABSTRACT

Background: Cancer Related Fatigue (CRF) is one of the most prevalent and distressing symptoms associated with cancer treatments. The exact etiology of CRF and its mechanisms are poorly understood. Cytokine dysregulation was hypothesized to be one of these mechanisms. Here, we explored the associations of soluble and extracellular vesicle (EV)-associated markers that include cytokines, heat shock proteins (hsp27, hsp70, hsp90), and neurotrophic factors (BDNF) with CRF.

Methods: Plasma was collected from men (n = 40) with non-metastatic prostate cancer receiving external beam radiation therapy (EBRT) at the start of the treatment, and three months after EBRT. CRF was assessed using the Functional Assessment of Cancer Therapy - Fatigue (FACT-F) from all participants. EVs were characterized via Nanoparticle Tracking Analysis, electron microscopy, and Western blot. Concentrations of EV-associated and soluble markers were measured with a multiplexed immunoassay system. Bivariate correlation analyses and independent T tests analyzed the relationships of CRF with the markers.

Findings: As CRF worsened, concentrations of EV-associated markers were upregulated. EV-associated fold changes of Eotaxin, hsp27, IP-10, MIP-3α, were significantly higher in fatigued participants compared to non-fatigued EBRT participants three months after treatment. This was not observed in soluble markers. Concentrations of EV-associated CRP and MCP-1, soluble survivin, IFNα2, IL-8, IL-12p70, and MCP-1 significantly correlated with lower (worsening) CRF scores at the start of and three months after treatment.

Interpretation: Concentrations of EV-associated markers increased in fatigued men with prostate cancer three months after EBRT. Both EV-associated and soluble markers correlated with worsening CRF. EV-associated markers, which have not been previously studied in depth, may provide additional insights and serve as potential biomarkers for CRF.

1. Introduction

Chronic fatigue is a debilitating condition that impairs the ability of patients to participate in personal and professional activities resulting in significant economic losses (Reynolds et al., 2004). Clinical heterogeneity in disease onset and divergent pathophysiology make it a difficult phenomenon to study (Sotzny et al., 2018). Here, we studied this behavioral consequence in a natural model with a known general cause and starting point. We investigated cancer-related fatigue (CRF) induced by radiation therapy with or without prior prostate cancer surgery.

CRF has been reported by 30%–60% of patients undergoing cancer therapies, where a third of these patients continue to experience CRF months to years after completing cancer therapy (Bower, 2014). CRF is defined by the National Comprehensive Cancer Network (NCCN) as a "distressing, persistent, and subjective sense of physical, emotional, and/or cognitive tiredness or exhaustion related to cancer or cancer treatment that is not proportional to recent activity and interferes with usual functioning" (National Comprehensive Cancer Network, 2020).

* Corresponding author. Section on Intercellular Interactions, Eunice Kennedy-Shriver National Institute of Child Health and Human Development, National Institutes of Health, Bethesda, MD, USA.
E-mail address: margolil@mail.nih.gov (L. Margolis).

https://doi.org/10.1016/j.bbih.2020.100140
Received 1 September 2020; Accepted 4 September 2020
Available online 25 September 2020

NCCN recommends early intervention to help moderate long-term economic, social, and psychological burdens that CRF exerts on these patients. This necessitates a need to identify early quantitative biomarkers that may recognize patients at greatest risk for long-term CRF.

Impaired immune response has been implicated in the etiology of CRF (Bower, 2014; Feng et al., 2017a, 2017b; L. Saligan et al., 2015), and thus, immune parameters are potential biomarkers. Upregulated cytokines that persisted for months and years after therapy have been suggested as biomarkers for CRF. These include: tumor necrosis factor-related apoptosis-inducing ligand (TRAIL) (Feng et al., 2017a, 2017b), brain-derived neurotrophic factor (BDNF) (Saligan et al., 2016), interleukin (IL)-6, C-reactive protein, IL-1β (Bower et al., 2009), IL-3, IL-8, IL-9, IL-10, IL-16, interferon-γ, interferon-α2, and stromal derived factor α (Feng et al., 2017a, 2017b). While several cytokines were reported to decrease at two months after treatment (Bower et al., 2009), TRAIL was reported to increase in CRF patients, one and two years post external beam radiation therapy (EBRT).

The above-cited studies observed these markers in the soluble fraction of peripheral blood. Recently, it was found that some of these cytokines are associated with extracellular vesicles (EVs) (Fitzgerald et al., 2018). EVs are small lipid bilayer particles ranging from 40 nm to 1000 nm in size and are found in body fluids including: blood, urine, breast milk, and saliva (Raposo and Stoorvogel, 2013). EVs include exosomes, microvesicles, and apoptotic bodies, which have different routes of biogenesis. EVs have the capacity to exchange proteins, lipids, and genetic material between cells, and play a potent role in intercellular communication (Raposo and Stoorvogel, 2013; Yáñez-Mó et al., 2015).

Several studies described EV-associated (surface-bound or encapsulated) cytokines related to HIV-1 infection (Mercurio et al., 2020) and traumatic brain injury (Gill et al., 2018). Researchers suggested that cytokines found on the surface of EVs may serve as "bar codes" that facilitate the communication between cells through receptor molecules (Margolis and Sadovsky, 2019). In this exploratory study, we assessed not only EV-associated and soluble cytokines, but also, heat shock proteins and a neurotrophic factor, which, for the purposes of this paper, we will designate as EV-associated and soluble markers.

This study is unique because it examines previously published as well as new markers of CRF, in both soluble and EV-associated forms, at three months post treatment to identify early markers for the development of CRF post treatment. We hypothesized that concentrations of EV-associated and soluble immune markers correlate with the severity of CRF. In this study, we test this hypothesis by investigating the relationship between EV-associated and soluble inflammatory and neurotrophic markers with the levels of CRF in patients with prostate cancer that received EBRT at two time points: baseline (start of EBRT) and three months after treatment.

2. Methods

2.1. Study design and participants

A descriptive, one-group, prospective cohort was used in this study under an NIH-approved protocol (NCT00852111). The clinical trial is registered in clinicaltrials.gov. We recruited men with non-metastatic prostate cancer who were scheduled to receive EBRT. Blood samples and questionnaires were collected at the start of EBRT (T1) and three months after completion of EBRT (T2). The inclusion criteria included: men: ≥18 years of age, scheduled to receive EBRT either by 3D conformal or intensity modulated radiation therapy techniques that were not anticipated to change during the course of the study, with or without concomitant androgen deprivation therapy, and with written informed consent demonstrated by 80% passing score on the consent quiz.

Exclusion criteria included: progressive or unstable disease of any body system causing clinically significant fatigue (e.g. lung disease, ischemic heart attack), systemic infections (e.g. HIV), history of major depression, bipolar disease, psychosis, or alcohol abuse within five years, uncorrected hypothyroidism and anemia, chronic inflammatory disease, use of tranquilizers, steroids, nonsteroidal anti-inflammatory drugs, and presence of previous or secondary malignancies or concurrent chemotherapy with radiation.

Because this is an exploratory study to gather preliminary data on EVs in CRF, we used the convenience sampling method from the current ongoing trial.

2.2. Procedures

All questionnaires and blood samples were collected and stored following National Institutes of Health standard operating procedures from 2009 to 2014.

Participants received EBRT, using an intensity modulated radiation therapy (IMRT) technique, five days a week for a total dose of 70–80 Gy and 38–42 fractions, at the National Cancer Institute Radiation Oncology Branch, NIH Clinical Center. Patient data was collected at the start of EBRT (T1) and three months after treatment was completed (T2).

2.3. Variables

Study variables included: CRF scores (primary outcome), socio-demographic and clinical variables (co-variates), and concentrations of 45 markers including cytokines, heat shock proteins, and a neurotrophic factor (secondary outcomes).

2.4. Data sources

The Functional Assessment Cancer Therapy- Fatigue (FACT-F) Questionnaire. FACT-F is a 13-item validated questionnaire (Yellen et al., 1997) and scores ranged from 0 to 52, with lower scores denoting higher fatigue levels. A change in FACT-F scores of ≥3 points between the two time points (T1-T2) was considered clinically meaningful based on previously published criteria (Cella et al., 2002). This phenotypic approach was successful in identifying biologic correlates of CRF in previous longitudinal reports (Feng et al., 2017a; Feng et al., 2017b); therefore, it was used to classify the EBRT cohort into fatigued and non-fatigued groups. FACT-F scores were used as continuous variables in exploring the relationships of EV-associated and soluble markers with CRF.

Sample Preparation. Whole blood samples were collected from study participants using EDTA tubes at both time points. Plasma was separated from whole blood, aliquoted in 250 μl, and stored in -80 °C freezers until batch analysis. The plasma was thawed on ice and platelet poor plasma (PPP) was obtained by two rounds of centrifugation at 3000 g for 15 min (Vagida et al., 2017). PPP was immediately processed using ExoQuick™ for plasma (SystemBio, Palo Alto, CA), according to the manufacturer's instructions. The supernatant (EV-free) was collected and the pellet was resuspended into their original volume of 250 μl of sterile phosphate-buffered saline (PBS). The supernatant and EV fractions were prepared the same day for multiplexed bead-based assays, and unused EV fractions were stored at -80 °C.

2.5. Characterization of EVs

Using the minimal information guidelines developed by the International Society of Extracellular Vesicles (Théry et al., 2018), Western blot and transmission electron microscopy (TEM) were conducted to verify the presence of EVs.

Transmission Electron Microscopy. Freshly isolated EVs were prepared using ExoQuick™, as described above. The resuspended pellets were subsequently purified using Exo-Spin purification columns (EX02) that exploit size exclusion chromatography (Cell Guidance System, St. Louis, MO). All samples were prepared for negative staining by the following procedures: 4 μl of exosome sample (diluted 40x in distilled water) were allowed to adsorb on the surface of a formvar/carbon, 200

mesh cooper grid (Electron Microscopy Sciences, Hatfield, PA) for 1 min. Excess liquid was removed using a piece of clean filter paper and allowed to dry. Next, 4 μl of filtered aqueous 3% uranyl acetate (UA) were applied for 20 s on the grid and the excess UA was removed using filter paper. The grid was air-dried before being examined in a JEOL-1400 Transmission Electron Microscope operating at 80 kV. Images were acquired on an AMT BioSprint-29 camera.

Protein quantification. Isolated EVs in 100 μl of PBS were lysed using 10 μl of 10x RIPA (Abcam, Cambridge, MA) and 1 μl of 100x protease inhibitor (Cell Signaling, Danvers, MA), vortexed for 15 s and placed at room temperature to allow full lysis. Samples were centrifuged at 16,000 g × 20 min at 4 °C to remove extra debris. Protein quantification was performed using Take3 micro-volume plate with BioTek Synergy H1 multi-mode reader (Biotek, Winooski, VT). Briefly, 2 μl of each sample were loaded in duplicate and measured at 280 nm absorbance and quantitated using Gen5 software pre-programmed protocols.

Western blot. EV fractions prepared using procedures described above and stored at -80 °C were thawed and analyzed for the presence of EV markers (CD81, TSG101, and Calnexin). Two samples per cohort (EBRT-T1, EBRT-T2) were loaded at 5–10 mg/ml into a 4–20% pre-cast polyacrylamide gel (Bio-Rad Laboratories, Hercules, CA). Standard Sodium Dodecyl Sulfate-polyacrylamide gel electrophoresis (SDS-PAGE) was performed to separate proteins based on molecular weight and transferred onto polyvinylidene difluoride (PVDF) membranes. The membranes were blocked with 5% milk in Tris Buffered Saline with 0.05% Tween 20 for 45 min. Following blocking and washing, membranes were incubated with anti-TSG101 at 0.2 μg/ml, anti-CD81 at 0.2 mg/ml, and anti-Calnexin at 0.2 μg/ml (Thermo Fisher Scientific, Waltham, MA) overnight at 4 °C. The following day, membranes were washed and incubated with goat peroxidase-conjugated anti-mouse IgG secondary antibody at 1:3000 dilutions (Bio-Rad). Peroxidase activity and digital images were detected by using Clarity™ enhanced chemiluminescence substrate and V3 Western Workflow™ (Bio-Rad).

2.6. EV size and concentration

Nanoparticle Tracking Analysis (NTA). EV samples were serially diluted 1:1000 with PBS. Samples were analyzed on a NanoSight NS300 (Malvern, UK) using NTA software (Malvern) (screen gain 2, camera Level 12, detection threshold 7). To generate averaged particle size and EV concentrations, each sample was analyzed by 3 video captures of 60 s. The values derived from control PBS + ExoQuick^{TM} were deducted from totals.

Multiplexed Bead-Based Assays. Two in-house multiplexed bead-based assays were developed to measure 45 markers. The first assay, which was previously published (Fitzgerald et al., 2018), measured 33 cytokines: IL-1α, IL-1β, IL-2, IL-4, IL-6, IL-7, IL-8, IL-10, IL-12p70, IL-13, IL-15, IL-16, IL-17, IL-18, IL-21, IL-22, IL-33, Calgranulin A (S100A8), Eotaxin (CCL11), granulocyte-macrophage colony-stimulating factor (GM-CSF), growth-regulated alpha (GRO-α or CXCL1), interferon-γ (IFN-γ), interferon-γ-induced protein (IP-10 or CXCL10), interferon-inducible T-cell alpha chemoattractant (ITAC or CXCL11), macrophage colony-stimulating factor (M-CSF), monocyte chemoattractant protein-1 (MCP-1 or CCL2), monokine induced by IFN-γ (MIG or CXCL9), macrophage inflammatory protein-1α (MIP-1α or CCL3), MIP-1β (CCL4), MIP-3α (CCL20), regulated on activation normally T-cell expressed and secreted (RANTES or CCL5), transforming growth factor-β (TGF-β), and tumor necrosis factor-α (TNF-α). The second assay measured an additional 12 proteins: eight cytokines/inflammatory markers (IL-3, IL-6 receptor (R), IL-9, TNF- related apoptosis-inducing ligand (TRAIL), C-reactive protein (CRP), stromal derived factor (SDF), survivin, and interferon alpha 2 (IFNα2)), one neurotrophic protein (brain-derived neurotrophic factor (BDNF)), and three heat shock proteins (hsps) (hsp27, hsp70, and hsp90).

Antibody pairs and standards were purchased from R&D Systems (Minneapolis, MN), except for IL-3, IL-4, IL-9, IFNα2 (Biolegend, San Diego, CA), IL-21 (Thermo Fisher), and hsp27, hsp70, hsp90 (AssayPro, St. Charles, MO; Ray Biotech, Peachtree Corners, GA; and Origene, Rockville, MD). Reagents were tested to ensure there was no cross-reactivity or interference, to optimize dynamic ranges, and to ensure optimal sensitivity. Specific buffers were employed to reduce non-specific binding and to account for the plasma matrix.

Beads were prepared by coupling monoclonal capture antibodies to Magplex microspheres (Luminex, Austin, TX) according to manufacturer's recommendations. Samples (plasma free of EVs and EV fractions) and standards were diluted in ProCarta Universal Assay Buffer (Thermo Fisher). As mentioned in the sample preparation, EV pellets were resuspended back to their original volume prior to measurement. Standards and EV fractions were measured before and after lysis with Triton X-100 (0.1% final concentration), as previously described (Fitzgerald et al., 2018). Samples from different groups of donors were randomized across all plates and samples for each donor were run on the same plate.

Samples/standards were incubated with beads overnight at 4 °C, washed and incubated at room temperature for 1 h with biotinylated antibodies specific to each protein in PBS containing 1% serum of host species of the antibodies. Plates were washed and incubated with 16 μg/ml streptavidin-phycoerythrin for 30 min, washed and resuspended in PBS for analysis on a Luminex 200 instrument set to acquire 100 events per analyte.

Analysis of multiplexed data was performed using Bioplex Manager software (Biorad). Final concentrations of analytes in EV-free supernatants were adjusted for dilution by ExoQuick^{TM} reagent. Cytokine concentrations on EV surface were determined by measurement on intact EV fractions (no detergent), and EV internal cytokines were determined by subtracting EV surface bound cytokines from EV total (detergent lysed EVs). Standard curves and lower limits of detection (LLOD) were determined using 5P logistic regression and the curve optimization feature; curves between all plates were compared between batches for consistency (see Supplemental Table 1).

2.7. Statistical analysis

Statistical analysis was conducted using IBM SPSS Grad pack 24.0. Descriptive statistics were run for means, standard deviations, and frequency distributions for all demographic, clinical, and outcome variables. Marker concentration values were transformed to logarithm base 10 (log 10 concentration). The associations of CRF scores with EV-associated and soluble markers were assessed via bivariate partial correlation test.

Data Discovery. Transformed log 10 (L10) marker concentrations values were used for analyses and data presentation needs in the JMP version 14 Statistical Discovery Software (SAS headquarters, Cary, NC). Hierarchical Clustering (HC) and heat maps were created for EV and soluble average log 10 marker concentrations for four groups: non-fatigued T1, non-fatigued T2, fatigued T1 and fatigued T2. Averaged EV log 10 marker concentrations were submitted to a mean centered hierarchical clustering analysis in JMP using the Ward distance matrix measures. The dendrogram was colored at the breaking nodes of five clusters to designate those EV markers within the cluster showing similar expression patterns. Averages of soluble markers were displayed in a heatmap using the same clustering display order as that of the EV-associated markers to investigate expression patterns evenly across the two marker types.

The log 10-fold change (L10FC deemed delta log 10 values) was calculated for each marker between T2 versus T1 concentrations for both the EV and soluble fractions. An independent t-test was calculated between fatigued and non-fatigued groups on the delta log 10 values to determine significance.

3. Results

This ongoing trial recruited 315 patients to date and enrolled 141 participants. Fifteen participants withdrew from the study due to changes

Table 1
Clinical and demographic characteristics.

	Fatigued (n = 16)	Non-Fatigued (n = 24)	*P* value
Age (y)	66.6 (7.5)	67.04 (7.4)	0.904
BMI	32.3 (4.9)	28.12 (3.4)	0.003
Radiation Dose (IMRT dose in Grey)	7611 (130.7)	7657 (162)	0.381
Race/Ethnicity			0.708
White	75.00%	62.50%	
Black/African American	18.80%	29.20%	
Asian	6.30%	4.20%	
Hispanic		4.20%	
T -stage			
T0			
T1c	31.30%	33.30%	
T2a	25.00%	50.00%	
T2b	12.50%		
T2c	6.30%	4.20%	
T3a	6.30%	12.50%	
T3b	18.80%		
Gleason Score Categories			
3 + 3 = 6	12.50%	4.20%	
3 + 4 = 7	43.80%	25.00%	
4 + 3 = 7	18.80%	8.30%	
4 + 4 = 8	12.50%	41.70%	
5 + 4 = 9	6.30%	4.20%	
4 + 5 = 9	6.30%	12.50%	
ADT	75.00%	83.00%	0.5
Surgery (prostatectomy)	12.50%	8.30%	0.7
Hemoglobin (g/dL) Baseline	13.85 (0.8)	14.2 (1.2)	0.632
RBC (mcL)_Baseline	4.6 (0.3)	4.6 (0.5)	0.985
PSA (ng/mL)	10.15 (25.5)	6.3 (7)	0.487
Hemoglobin (g/dL) T2	13.15 (1)	4.2 (0.53)	0.492
RBC (mcL)_T2	4.3 (0.31)	12.8 (1.2)	0.35

Abbreviations: BMI = body mass index, ADT = androgen deprivation therapy, HB = hemoglobin, RBC = red blood cells, PSA = prostate specific antigen, IMRT = intensity modulated radiation therapy.

in their cancer diagnosis (n = 3), non-compliance to study procedures (n = 6), or diagnosis of a new medical condition (n = 6). A total of 40 patients with complete FACT-F scores and available plasma samples at the start of radiation and three months after treatment were selected to address the exploratory aims of this project.

All clinical and demographic variables were similar between fatigued and non-fatigued EBRT groups except for body mass index (BMI). BMI was significantly higher in the fatigued group ($p = 0.003$). No missing data was found in this project due to the convenience sampling method used. Clinical and demographic characteristics of all participants are presented in Table 1.

CRF. Compared to baseline (T1), 40% of patients (n = 16/40) reported worsening fatigue (change in fatigue scores of ≥3) at three months (T2) after EBRT. Wilcoxon signed rank test showed a significant decrease in CRF scores (worsening) in fatigued ($p < 0.0001$) and increase in scores (improving CRF) in non-fatigued group ($p = 0.001$) (Fig. 1).

EV characterization and validation was performed following ISEV guidelines (Théry et al., 2018).

Western blot. We tested three EV markers: CD81 (non-tissue specific tetraspanin), TSG101 (cytosolic protein), and Calnexin (endoplasmic reticulum protein) to validate the presence of EVs after ExoQuick™ isolation. We confirmed the presence of CD81 and TSG101 while showing the absence of Calnexin, which indicates that the EV population falls into a smaller subtype of EVs (Fig. 2).

Transmission Electron Microscopy (TEM). Representative image of vesicles isolated from the plasma of patient with prostate cancer using ExoQuick™. The images demonstrate cup-shaped vesicles with lipid bilayers. (A-wide angle) (B-close up image) (Fig. 3).

Nanosight. Size and concentration of vesicles were characterized using NTA. The average concentration of EVs was 1.05E+12 (6.46E+11) particles per ml at T1 and 1.14E+12 (11.21). The average sizes of EVs in the EBRT group at T1 was approximately 135.7 (15.4) nm and 135.3 (56.2) nm at T2.

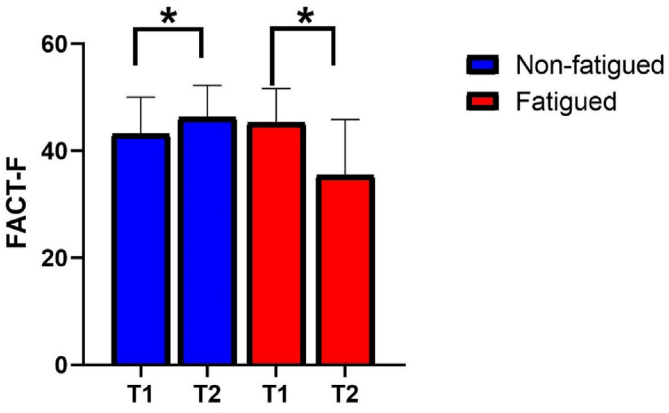

Fig. 1. Change in CRF scores from T1 to T2 (EBRT group n = 40). In the external beam radiation therapy (EBRT) group, 40% of patients (n = 16/40) reported worsening cancer-related fatigue (CRF) at T2. Wilcoxon signed rank test showed decrease in FACT-F scores in fatigued cohort ($p < 0.0001$) and increase in FACT-F scores in non-fatigued cohort ($p = 0.001$). *denotes statistical significance. Validation of the Presence of EVs.

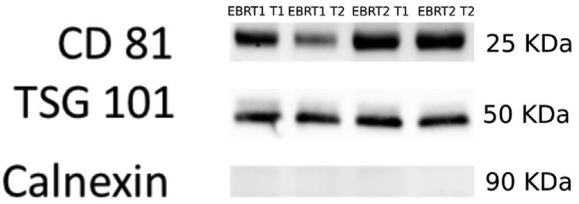

Fig. 2. Western blot validation of presence of EVs. EVs isolated from the plasma of external beam radiation therapy (EBRT) men demonstrated the presence of EV markers (CD81, TSG101) while showing absence of calnexin. EBRT1 = patient 1, EBRT2 = patient 2; T1 (at the start of EBRT), T2 (3 months post EBRT).

Inflammatory and Neurotrophic Markers.

Soluble vs. EV-associated Markers. Inflammatory and neurotrophic markers were measured in EV-associated fractions and in supernatants (soluble) of plasma samples. Concentrations of EV internal on average were small, thus EV total referred to as EV-associated (EV surface + EV internal) was used for ease of data representation (Supplemental Table 2). Soluble and EV-associated markers had different concentrations as illustrated in heat maps (Fig. 4). For example, at T2, markers associated with the fatigued EBRT group which included Calg-A, GM-CSF, IL-6, M-CSF, ITAC, IL-1α, IL-7, IP-10, IL-13, IL-8, IL-21, TNF-α, IL-4, TGF-β, MIP-3α were more concentrated in EVs compared to corresponding soluble markers.

Fatigued and non-fatigued EBRT groups.

We examined the change in concentrations of markers from T1 to T2 (delta log 10 values) between fatigued and non-fatigued subjects (Logarithm base 10 (T2-T1), a positive L10FC indicates higher cytokine concentration at T2 than at T1 (i.e. cytokine expression increased after treatment) and a negative L10FC indicates a lower cytokine expression at T2 than at T1 (i.e. cytokine expression decreased after treatment)). Two group independent T-tests showed that EV-associated L10FC's of Eotaxin ($p = 0.027$), hsp27 ($p = 0.042$), IP-10 ($p = 0.047$), MIP-3α ($p = 0.0092$) were significantly higher in fatigued compared to non-fatigued EBRT men, which was not observed in the soluble fraction. EV-associated L10FC IL-3 was significantly lower in fatigued versus non-fatigued EBRT men ($p = 0.047$). Soluble L10FC survivin was higher ($p = 0.049$) in fatigued versus non-fatigued EBRT men (Fig. 5). All L10FC cytokine

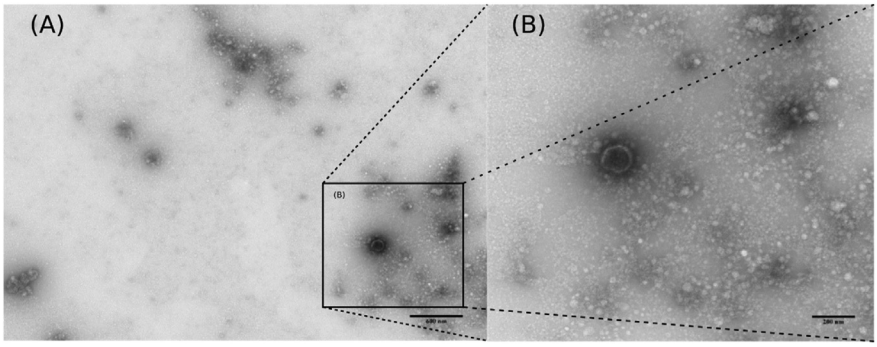

Fig. 3. Representative EM Image A) Wide angle, Direct Mag:10000x, HV = 80 kV, Scale: 600 nm B) Close up image, Direct Mag:25000x, HV = 80 kV, Scale:200 nm.

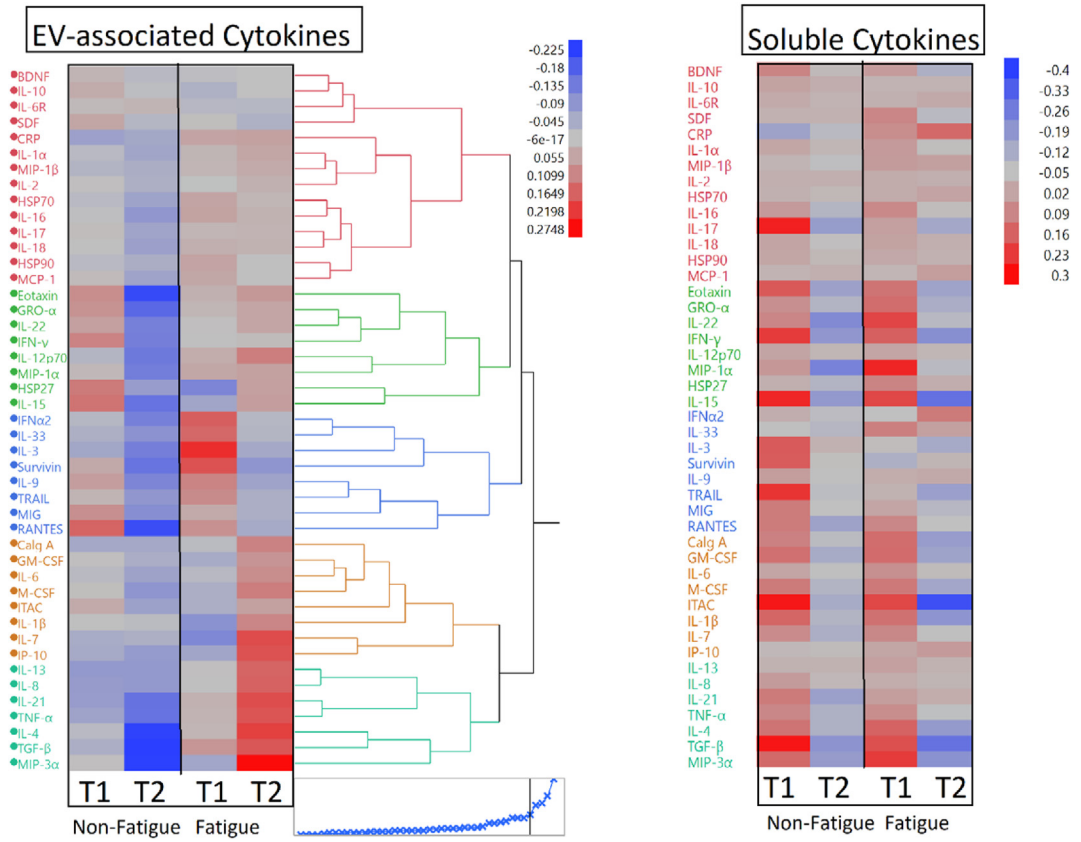

Fig. 4. Hierarchical Clustering and Heat Map Comparison for EV-associated and Soluble Cytokines. Average EV-associated cytokine expression (left panel) showed five clusters of like markers with like cytokine expressions. Heat map of soluble markers (right panel) in the external beam radiation therapy (EBRT) group showed differences in concentrations of individual markers based on cancer-related fatigue (CRF). Abbreviations: T1 = at the start of radiation, T2 = three months post EBRT.

changes were tested with an Analysis of Covariance (ANCOVA) in order to investigate an interaction covariate effect of BMI (continuous variable) and binary fatigue (categorical). None of the significant markers had significant interaction with BMI (Fig. 6).

3.1. Correlations between immune markers and CRF scores

We ran partial correlations between L10 concentrations of markers and FACT-F scores while controlling for BMI. At the start of radiation (T1), in the fatigued EBRT group, EV-associated MCP-1 ($p = 0.038$) and soluble survivin ($p = 0.024$) negatively correlated with FACT-F scores (worsening CRF) (Table 2).

At T2, in the fatigued EBRT group, EV-associated CRP ($p = 0.010$) correlated with lower FACT-F scores, while BDNF ($p = 0.014$) positively correlated with FACT-F scores. Soluble IFNα2 ($p = 0.020$), IL-8 ($p = 0.011$), IL-12p70 ($p = 0.001$), and MCP-1 ($p = 0.045$) levels correlated with lower FACT-F scores while controlling for BMI (Table 3).

4. Discussion

Here, we explored the associations of EV-associated and soluble markers with CRF. We found that: (1) L10FC of EV-associated Eotaxin, hsp27, IP-10, MIP-3α and soluble survivin were upregulated in fatigued cohort compared to non-fatigued, and (2) concentrations of L10 EV-associated CRP, MCP-1, and soluble survivin, IFNα2, IL-8, IL-12p70 and MCP-1 were negatively correlated, with FACT-F scores (worsening CRF). To our knowledge, this is the first paper to explore the relationships of EV-associated markers and CRF.

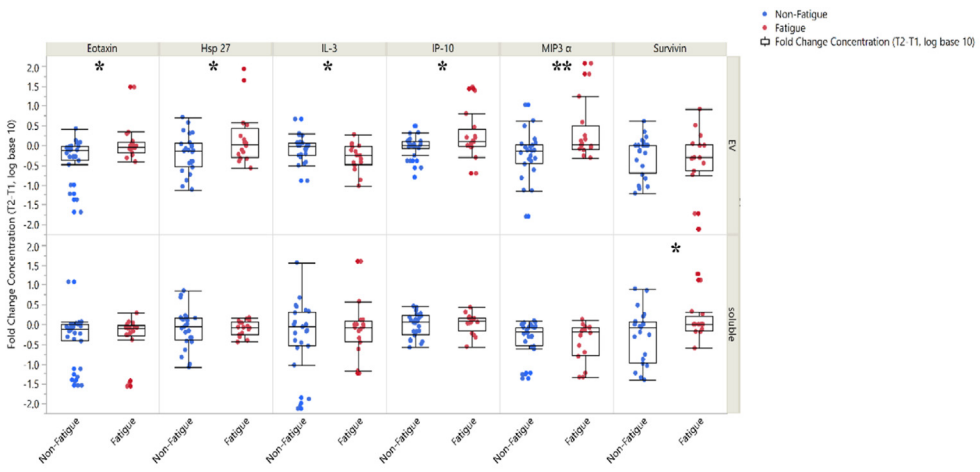

Fig. 5. One-way Bivariate Plot of delta log 10 values between Non-Fatigue and Fatigue groups. Log10FC expression of six cytokines plotted. Two group independent t-test examining significant change in concentrations of cytokines from T1 to T2 in fatigued (red) (n = 16) and non-fatigued (blue) (n = 24) men: Eotaxin $p = 0.027$, hsp27 $p = 0.042$, IL-3 $p = 0.047$, IP-10 $p = 0.047$, MIP-3α $p = 0.0092$, Survivin $p = 0.049$. (For interpretation of the references to color in this figure legend, the reader is referred to the Web version of this article.)

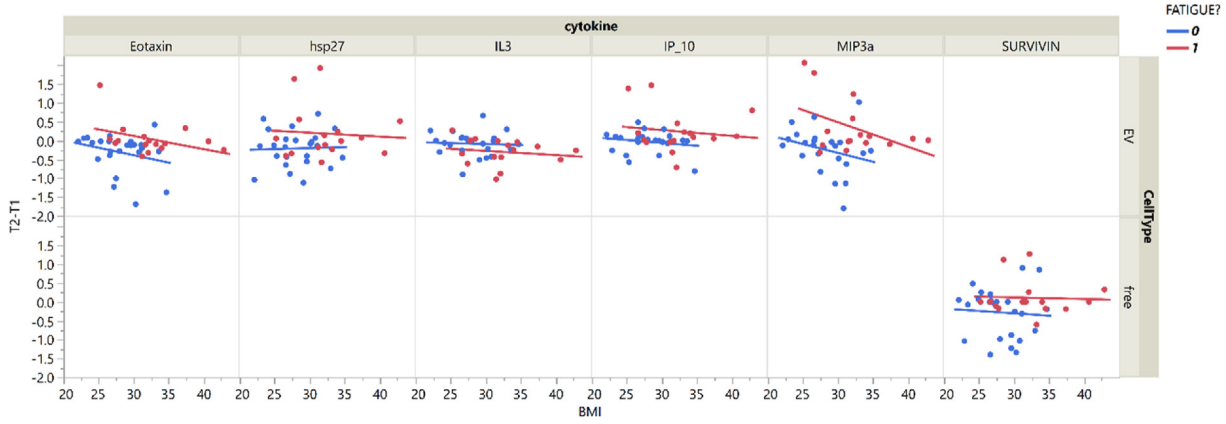

Fig. 6. Bivariate Plot of BMI and Log10FC of cytokines (T2-T1). BMI (x-axis) versus delta 10 values (y-axis) for fatigue (red) and non-fatigue (blue) for seven cytokines found to be significantly different. Fitted regression line for each group. The BMI*fatigue interaction p value for each of the 6 cytokines are as follows for EV: Eotaxin $p < 0.9$, hsp27 $p < 0.74$, IL-3 $p < 0.9$, IP-10 $p < 0.9$, MIP-3α $p < 0.72$; and for EV_free (soluble): Survivin $p < 0.87$. These results indicate that there is no BMI effect on cytokine fold changes between fatigue and non-fatigue. (For interpretation of the references to color in this figure legend, the reader is referred to the Web version of this article.)

We reported upregulation of L10FC of EV-associated Eotaxin, IP-10, MIP-3α, and hsp27. Eotaxin, IP-10, and MIP-3α, are members of the chemokine family, while hsp27 is a member of the heat shock protein family. Chemokines are small proteins (60–100 amino acids) that structurally resemble cytokines and are grouped into inflammatory and homeostatic subfamilies (Deshmane et al., 2009). Chemokines are released by a variety of cells where they guide cells of the immune system to where they are needed most (Arango Duque and Descoteaux, 2014). EV-associated hsp27 has been shown to stimulate NFkβ activation and release IL-10 *in vitro* contributing to anti-inflammatory effects (Shi, Ulke-Lemée, Deng, Batulan, & O'Brien, 2019). We hypothesize that, in our study, CRF is related to the upregulation of inflammatory chemokines and upregulation of anti-inflammatory hsp27, which could be serving as a protective mechanism. Similar observations were previously described in muscle fatigue in the geriatric population (Beyer et al., 2012).

L10FC of soluble survivin was higher at T2 in the fatigued cohort compared to non-fatigued participants. Survivin belongs to the family of the inhibitor of apoptosis (IAO) and is increased during G2/M cell cycle phase (Rafatmanesh et al., 2020). Increased expression of survivin promotes resistance to apoptosis and has been linked to a variety of different cancers (Rafatmanesh et al., 2020) including prostate cancer (Zhang et al., 2010).

Previously, soluble survivin was not described in CRF, but it has been implicated in autoimmune diseases (Gravina et al., 2017) and plays a role in the innate immune system; more specifically it is highly expressed in immature neutrophils (Altznauer et al., 2004). Researchers note that expression of survivin is not only overexpressed in cancers, but also other pathologic inflammatory conditions (Altznauer et al., 2004); thus, it could be indicative of an overall inflammatory process.

We also performed correlation analyses between FACT-F scores and concentrations of EV-associated and soluble markers in the fatigued individuals. We showed that EV-associated CRP and MCP-1, as well as soluble IL-8, survivin, IL-12p70 and MCP-1 significantly correlated with worsening CRF, suggesting both the EV-associated and soluble markers can be informative to explain the pathobiology of CRF. EV-associated BDNF was positively correlated with CRF meaning that as the fatigue scores increased (improved), the concentration of BDNF increased.

In our analysis EV-associated MCP-1 negatively correlated with CRF scores at T1, while soluble MCP-1 correlated at T2. It is interesting that MCP-1 was significant in either EV-associated or soluble fractions, but not in both at the same time point. MCP-1 is considered to be one of the key chemokines responsible for recruiting monocytes to the site of inflammation (Deshmane et al., 2009), promoting Th1 and Th2 response and has both pro- and anti-inflammatory functions (Trial et al., 2013). We hypothesize that at T1, the upregulation of this chemokine may be due to the stress of receiving the diagnosis and anticipating the start of the treatment and at T2, it may be contributing to the development of CRF.

Table 2
Correlation Between Markers and FACT-F scores at T1 in the Fatigued Group-[a]Controlling for BMI (n = 16).

	EV	p value	Soluble	p value
	Correlation		Correlation	
BDNF	0.040	0.887	0.074	0.792
CRP	-0.318	0.248	-0.508	0.053
HSP27	-0.273	0.325	0.184	0.513
HSP70	0.353	0.197	0.373	0.170
HSP90	0.076	0.788	0.139	0.621
IFNα2	-0.122	0.665	0.303	0.272
IL-3	0.105	0.709	-0.458	0.086
IL-9	-0.182	0.517	-0.364	0.182
IL-6R	-0.254	0.360	0.191	0.495
SDF	-0.396	0.144	0.079	0.781
Survivin	-0.458	0.086	-0.578[a]	0.024
TRAIL	-0.384	0.158	-0.201	0.472
IL-1α	0.101	0.721	0.140	0.619
IL-1β	0.146	0.604	0.215	0.442
IL-2	-0.312	0.258	0.158	0.573
IL-4	-0.062	0.825	0.446	0.096
IL-6	0.190	0.497	0.158	0.574
IL-7	0.054	0.847	0.493	0.062
IL-8	-0.484	0.068	-0.287	0.299
IL-10	NA	NA	NA	NA
IL-12p70	-0.340	0.216	0.180	0.522
IL-13	-0.462	0.083	0.199	0.476
IL-15	0.480	0.070	0.346	0.206
IL-16	-0.169	0.547	0.069	0.806
IL-17	0.165	0.558	-0.137	0.627
IL-18	0.117	0.678	-0.116	0.681
IL-21	-0.172	0.540	-0.093	0.741
IL-22	0.035	0.900	0.239	0.390
IL-33	0.189	0.500	0.199	0.476
Calg A	-0.462	0.083	0.244	0.382
Eotaxin	0.066	0.814	0.077	0.785
GM-CSF	0.169	0.548	0.296	0.284
GRO-α	0.111	0.694	0.337	0.219
IFN-γ	0.386	0.155	0.286	0.302
IP-10	-0.144	0.609	0.226	0.419
ITAC	0.153	0.587	0.153	0.585
M-CSF	0.038	0.894	0.338	0.218
MCP-1	-0.539[a]	0.038	-0.332	0.226
MIG	0.180	0.521	0.281	0.311
MIP-1α	0.324	0.240	0.121	0.666
MIP-1β	-0.300	0.277	-0.400	0.140
MIP-3α	0.262	0.346	0.035	0.901
TGF-β	-0.279	0.314	0.073	0.795
TNF-α	0.089	0.752	0.267	0.337
RANTES	0.090	0.751	-0.020	0.942

T1 = at the start of EBRT, EBRT = external beam radiation therapy,**$p < 0.01$, NA = not applicable.
[a] $p < 0.05$.

Table 3
Correlations Between Markers and FACT-F scores at T2 in the Fatigued Group-[a]Controlling for BMI (n = 16).

	EV	p value	Soluble	p value
	Correlation		Correlation	
BDNF	0.620[a]	0.014	0.442	0.099
CRP	-0.641[a]	0.010	-0.362	0.186
HSP27	0.051	0.856	0.475	0.074
HSP70	0.053	0.851	-0.239	0.391
HSP90	0.134	0.634	0.241	0.386
IFNα2	0.192	0.494	-0.593[a]	0.020
IL-3	0.474	0.074	0.029	0.920
IL-9	0.113	0.689	-0.365	0.181
IL-6R	-0.242	0.385	0.191	0.495
SDF	0.000	0.999	0.026	0.926
Survivin	0.064	0.821	-0.389	0.152
TRAIL	0.113	0.690	-0.028	0.922
IL-1α	-0.175	0.533	-0.512	0.051
IL-1β	-0.110	0.696	-0.328	0.233
IL-2	0.224	0.422	NA	NA
IL-4	0.179	0.523	-0.512	0.051
IL-6	-0.058	0.838	-0.209	0.456
IL-7	0.084	0.767	0.147	0.601
IL-8	-0.333	0.225	-0.636[a]	0.011
IL-10	-0.058	0.837	NA	NA
IL-12p70	-0.043	0.879	-0.747[b]	0.001
IL-13	0.151	0.591	NA	NA
IL-15	-0.035	0.902	-0.036	0.899
IL-16	0.097	0.731	0.034	0.905
IL-17	-0.246	0.377	-0.277	0.318
IL-18	-0.136	0.629	-0.082	0.773
IL-21	0.141	0.616	-0.247	0.376
IL-22	-0.017	0.952	-0.158	0.573
IL-33	-0.512	0.051	NA	NA
Calg A	0.222	0.426	0.066	0.815
Eotaxin	0.352	0.198	-0.075	0.789
GM-CSF	-0.070	0.803	0.009	0.974
GRO-α	-0.098	0.727	-0.105	0.710
IFN-γ	-0.191	0.494	-0.198	0.479
IP-10	0.098	0.727	-0.137	0.626
ITAC	0.198	0.480	-0.058	0.836
M-CSF	0.059	0.834	-0.095	0.737
MCP-1	-0.118	0.675	-0.524[a]	0.045
MIG	0.033	0.907	0.204	0.467
MIP-1α	0.026	0.926	-0.102	0.718
MIP-1β	-0.165	0.558	-0.402	0.137
MIP-3α	0.123	0.663	-0.006	0.984
TGF-β	0.044	0.878	-0.512	0.051
TNF-α	0.180	0.520	-0.138	0.623
RANTES	-0.060	0.831	0.062	0.826

T2 = three months after EBRT, EBRT = external beam radiation therapy.
[a] $p < 0.05$.
[b] $p < 0.01$, NA = not applicable.

CRP is a nonspecific acute phase protein elevated in inflammatory conditions (Pepys and Hirschfield, 2003). In our study, EV-associated CRP correlated with CRF, while soluble CRP did not. Similarly, a study with breast cancer survivors four years post survival, showed that high sensitivity CRP (hsCRP) correlated with CRF (Orre et al., 2011). Of note, we investigated CRP not hsCRP, and EV-associated CRP was more enriched in EVs compared to the soluble fraction in this study.

While the above-mentioned results are congruent with previously published data, our data on BDNF were different from those published by Saligan et al. (2016). We found that as the concentration of BDNF increased, CRF scores increased (improving CRF). A previous study (Saligan et al., 2016), found that BDNF was associated with worsening CRF. This apparent discordance may be explained by the difference in time points when BDNF was measured; while Saligan et al. measurements were performed midpoint of EBRT (around 19-21 daily sessions), we examined it three months after treatment completion.

Among the soluble markers, soluble IL-8, IFNα2, and IL-12p70 significantly correlated at T2. IL-8 is another chemotactic inflammatory cytokine that recruits neutrophils, basophils, and T cells to the site of infection (Murphy and Weaver, 2016). IFNα2 is part of the type I interferon family used for antitumor therapy (Paul et al., 2015). Both IL-8 and IFNα2 have been previously correlated with chronic CRF from baseline to one year after treatment measured at midpoint of EBRT (Feng et al., 2017a, 2017b).

IL-12p70 is a heterodimeric cytokine that consists of p35 and p40 subunits and belongs to the family of IL-12 related cytokines (Liu et al., 2005) and is a pro-inflammatory cytokine that facilitates Th1 differentiation (Vignali and Kuchroo, 2012). IL-12p70 was significantly upregulated and suggested to be a good predictor for chronic fatigue syndrome (CFS) in women with CFS compared to healthy women (Fletcher et al., 2009). In our study, IL-12p70 had a significant correlation with lower CRF scores indicating that as the fatigue worsened, the levels of IL-12p70 increased. Similarly, in women with chronic fatigue syndrome, IL-12p70 was significantly upregulated compared to healthy women (Fletcher et al., 2009).

Peripheral inflammation has been linked to severe behavioral consequences like CRF (Dantzer et al., 2014). Immune activation in general and inflammation in particular are associated with upregulation of many

cytokines. We hypothesize that cancer therapies, particularly EBRT, trigger alteration of the cytokine system that leads to CRF. Immune activation, manifested by increases in soluble and EV-associated markers, alters cell-cell communications. Our findings provide new insight into relations between immunity and CRF and are in agreement with earlier reports on the role of EV-associated markers in the context of other pathologies such as bacterial endotoxin release (McDonald et al., 2014), traumatic brain injury (Gill et al., 2018), and HIV infection (Mercurio et al., 2020).

Our study has several limitations. The sample size may not be large enough to reveal significance for the changes in some immune factors, which can be missed in the present work. Plasma samples were not collected after fasting or at a fixed time of the day, which may affect the concentrations of cytokines (Witwer et al., 2013). Samples were collected from 2009 to 2014 and while they were properly stored, some potential variability can be attributed to the difference in sample storage time. Our isolation method did not discriminate between different EV populations (e.g., exosomes, microvesicles) that may differentially affect CRF. Our assays cannot distinguish whether increase in protein concentration may be due to an increase in EV numbers or due to increase in specific EV subtypes that may carry that protein. It is likely that EV concentration is increased related to the disease process, but it is also plausible that particular EV subtypes are enriched in plasma. Thus, future investigations exploring specific EV subtypes can strengthen EV research in CRF. In addition, EV internal (EV lysed) had smaller concentrations than EV surface, so we combined the two compartments as EV total for ease in data reporting. We hypothesized that cytokines released in association with EVs may be released in lower concentrations because other proteins on the EV surface may target the cytokine to particular cell types and thus less cytokine is needed compared to the soluble compartment where a lot of cytokines must be released in order to find the right cell with specific cell receptors.

A multiple comparisons correction was not conducted due to the small sample size and the exploratory nature of the project. Despite these limitations, to our knowledge, this was the first exploratory analysis of the relationships between EV-associated and soluble markers with CRF.

In summary, this study suggests that both EV-associated and soluble markers have the potential to identify patients at risk for CRF three months after treatment and serve as early screening parameters for CRF before the development of chronic CRF (>6 months post treatment). In particular, we found that EV-associated Eotaxin, IP-10, MIP-3α, and hsp27 and soluble survivin was upregulated 3 months after treatment completion in the fatigued cohort versus non-fatigued cohort. These findings may provide some understanding in the discrepancy in fatigue experiences post cancer treatment. Our correlation analyses found that EV-associated CRP, MCP-1, and soluble survivin, IFNα2, IL-8, IL-12p70 and MCP-1 were associated with worsening CRF scores at each time point; however, there was little overlap between which markers were elevated in the EV versus soluble compartments. Our study affirms the contribution of EVs in understanding the relationships of systemic processes like inflammation in behaviors like CRF. Further investigations of EV-associated proteins and cell-specific EVs can help clinicians understand the complex interplay of peripheral and central biomolecules responsible for the development and chronicity of symptoms. Future studies with larger sample sizes and longer follow-up times >6 months, should be conducted to confirm these initial EV-associated markers and to elucidate the physiological processes of chronic CRF.

Contributions

DS, WF, LM, LS, KK designed the study. DS and WF were involved in data acquisition. DS, JJB, and KK were involved in data analysis. All authors were involved in data interpretation. DS, WF, LS, JJB, and LM drafted the manuscript and all authors were involved in revising the manuscript for intellectual content. All authors participated in data interpretation, contributed to the manuscript, and approved final version.

Declaration of competing interest

The authors declare that they have no known competing financial interests or personal relationships that could have appeared to influence the work reported in this paper.

Acknowledgments

This study is supported by the National Institute of Nursing Research (NINR) and National Institute of Child Health and Human Development (NICHD), NIH. The authors thank Louis Dye for services provided with the Microscopy & Imaging Core- NICHD, NIH. Authors thank Dr. Vincenzo Mercurio for assistance with Western blots. Authors also thank Drs. Ann Berger, Paula Schulz, Kristin Dickinson, and Adam Case in mentoring and supervising dissertation project by DS.

Appendix A. Supplementary data

Supplementary data to this article can be found online at https://doi.org/10.1016/j.bbih.2020.100140.

Funding

National Institute of Nursing Research and National Institute of Child Health and Human Development. Trial is registered: https://clinicaltrials.gov/ct2/show/NCT00852111?term=Leorey+Saligan&recrs=ab&draw=2&rank=2.

References

Altznauer, F., Martinelli, S., Yousefi, S., et al., 2004. Inflammation-associated cell cycle–independent block of apoptosis by survivin in terminally differentiated neutrophils. J. Exp. Med. 199 (10), 1343–1354.
Arango Duque, G., Descoteaux, A., 2014. Macrophage cytokines: involvement in immunity and infectious diseases. Front. Immunol. 5 (491), 1–12.
Beyer, I., Njemini, R., Bautmans, I., et al., 2012. Inflammation-related muscle weakness and fatigue in geriatric patients. Exp. Gerontol. 47 (1), 52–59.
Bower, 2014. Cancer-related fatigue—mechanisms, risk factors, and treatments. Nat. Clin. Pract. Oncol. 11 (10), 597–609.
Bower Ganz, P., Tao, M.L., et al., 2009. Inflammatory biomarkers and fatigue during radiation therapy for breast and prostate cancer. Clin. Canc. Res. 15 (17), 5534–5540.
Cella, D., Eton, D.T., Lai, J.-S., et al., 2002. Combining anchor and distribution-based methods to derive minimal clinically important differences on the Functional Assessment of Cancer Therapy (FACT) anemia and fatigue scales. J. Pain Symptom Manag. 24 (6), 547–561.
Dantzer, R., Heijnen, C.J., Kavelaars, A., et al., 2014. The neuroimmune basis of fatigue. Trends Neurosci. 37 (1), 39–46.
Deshmane, S.L., Kremlev, S., Amini, S., et al., 2009. Monocyte chemoattractant protein-1 (MCP-1): an overview. J. Interferon Cytokine Res. 29 (6), 313–326.
Feng, L.R., Suy, S., Collins, S.P., et al., 2017a. The role of TRAIL in fatigue induced by repeated stress from radiotherapy. J. Psychiatr. Res. 91, 130–138.
Feng, L.R., Wolff, B.S., Lukkahatai, N., et al., 2017b. Exploratory investigation of early biomarkers for chronic fatigue in prostate cancer patients following radiation therapy. Canc. Nurs. 40 (3), 184–193.
Fitzgerald, W., Freeman, M.L., Lederman, M.M., et al., 2018. A system of cytokines encapsulated in extracellular vesicles. Sci. Rep. 8 (1), 1–11.
Fletcher, M.A., Zeng, X.R., Barnes, Z., et al., 2009. Plasma cytokines in women with chronic fatigue syndrome. J. Transl. Med. 7 (1), 96.
Gill, J., Mustapic, M., Diaz-Arrastia, R., et al., 2018. Higher exosomal tau, amyloid-beta 42 and IL-10 are associated with mild TBIs and chronic symptoms in military personnel. Brain Inj. 32 (11), 1359–1366.
Gravina, G., Wasén, C., Garcia-Bonete, M., et al., 2017. Survivin in autoimmune diseases. Autoimmun. Rev. 16 (8), 845–855.
Liu, J., Cao, S., Kim, S., et al., 2005. Interleukin-12: an update on its immunological activities, signaling and regulation of gene expression. Curr. Immunol. Rev. 1 (2), 119–137.
Margolis, L., Sadovsky, Y., 2019. The biology of extracellular vesicles: the known unknowns. PLoS Biol. 17 (7), 1–12.
McDonald, M.K., Tian, Y., Qureshi, R.A., et al., 2014. Functional significance of macrophage-derived exosomes in inflammation and pain. Pain 155 (8), 1527–1539.
Mercurio, V., Fitzgerald, W., Molodtsov, I., et al., 2020. Persistent immune activation in HIV-1 infected ex vivo model tissues subjected to antiretroviral therapy: soluble and extracellular vesicle-associated cytokines. J. Acquir. Immune Defic. Syndr. 84 (1), 45–53.
Murphy, K., Weaver, C., 2016. Janeway's Immunobiology. Garland science.

National Comprehensive Cancer Network, N., 2020. NCCN clinical practice guidelines in Oncology, cancer-related fatigue. https://www.nccn.org/store/login/login.aspx?ReturnURL=https://www.nccn.org/professionals/physician_gls/pdf/fatigue.pdf.
Orre, I.J., Reinertsen, K.V., Aukrust, P., et al., 2011. Higher levels of fatigue are associated with higher CRP levels in disease-free breast cancer survivors. J. Psychosom. Res. 71 (3), 136–141.
Paul, F., Pellegrini, S., Uzé, G., 2015. IFNA2: the prototypic human alpha interferon. Gene 567 (2), 132–137.
Pepys, M.B., Hirschfield, G.M., 2003. C-reactive protein: a critical update. J. Clin. Invest. 111 (12), 1805–1812.
Rafatmanesh, A., Behjati, M., Mobasseri, N., et al., 2020. The survivin molecule as a double-edged sword in cellular physiologic and pathologic conditions and its role as a potential biomarker and therapeutic target in cancer. J. Cell. Physiol. 235 (2), 725–744.
Raposo, G., Stoorvogel, W., 2013. Extracellular vesicles: exosomes, microvesicles, and friends. J. Cell Biol. 200 (4), 373–383.
Reynolds, K.J., Vernon, S.D., Bouchery, E., et al., 2004. The economic impact of chronic fatigue syndrome. Cost Eff. Resour. Allocation 2 (1), 4.
Saligan Lukkahatai, N., Holder, G., et al., 2016. Lower brain-derived neurotrophic factor levels associated with worsening fatigue in prostate cancer patients during repeated stress from radiation therapy. World J. Biol. Psychiatr. 17 (8), 608–614. https://doi.org/10.3109/15622975.2015.1012227.
Saligan, L., Olson, K., Filler, K., et al., 2015. The biology of cancer-related fatigue: a review of the literature. Support. Care Canc. 23 (8), 2461–2478.
Shi, C., Ulke-Lemée, A., Deng, J., et al., 2019. Characterization of heat shock protein 27 in extracellular vesicles: a potential anti-inflammatory therapy. Faseb. J. 33 (2), 1617–1630.
Sotzny, F., Blanco, J., Capelli, E., et al., 2018. Myalgic encephalomyelitis/chronic fatigue syndrome–evidence for an autoimmune disease. Autoimmun. Rev. 17 (6), 601–609.
Théry, C., Witwer, K.W., Aikawa, E., et al., 2018. Minimal information for studies of extracellular vesicles 2018 (MISEV2018): a position statement of the International Society for Extracellular Vesicles and update of the MISEV2014 guidelines. J. Extracell. Vesicles 7 (1), 1–43.
Trial, J., Cieslik, K.A., Haudek, S.B., et al., 2013. Th1/M1 conversion to th2/m2 responses in models of inflammation lacking cell death stimulates maturation of monocyte precursors to fibroblasts. Front. Immunol. 4, 287–296.
Vagida, M., Arakelyan, A., Lebedeva, A., et al., 2017. Flow analysis of individual blood extracellular vesicles in acute coronary syndrome. Platelets 28 (2), 165–173.
Vignali, D.A., Kuchroo, V.K., 2012. IL-12 family cytokines: immunological playmakers. Nat. Immunol. 13 (8), 722.
Witwer, K.W., Buzás, E.I., Bemis, L.T., et al., 2013. Standardization of sample collection, isolation and analysis methods in extracellular vesicle research. J. Extracell. Vesicles 2 (1), 1–25.
Yáñez-Mó, M., Siljander, P.R.-M., Andreu, Z., et al., 2015. Biological properties of extracellular vesicles and their physiological functions. J. Extracell. Vesicles 4 (1), 27066.
Yellen, S.B., Cella, D.F., Webster, K., et al., 1997. Measuring fatigue and other anemia-related symptoms with the Functional Assessment of Cancer Therapy (FACT) measurement system. J. Pain Symptom Manag. 13 (2), 63–74.
Zhang, M., Coen, J.J., Suzuki, Y., et al., 2010. Survivin is a potential mediator of prostate cancer metastasis. Int. J. Radiat. Oncol. Biol. Phys. 78 (4), 1095–1103.